

Chapter 5 PROPOSED SOLUTION

The proposed solution to provide a quick method to draw a skeleton from motion capture data is presented in this chapter. The main contribution to the state of the science is the thorough analysis of the previously fastest sphere-fitting technique and the subsequent improvement of the answer.

5.1 Unbiased Generalized Delogne-Kása Estimator

The estimator explained in this chapter is asymptotically unbiased. Asymptotically unbiased is defined as an inversely proportional relationship with the sample count:

$$(170) \quad E(\hat{q}) = q_0 + O\left(\frac{1}{N}\right)$$

where q_0 is the parameter that the estimator is trying to estimate. This basically says that the estimator is expected to get closer to the true answer if more samples are taken. From the previous discussion in Section 4.1.5, it was shown that the GDKE estimators for center and radius do not satisfy this requirement. Our algorithm uses a simple substitution that turns the GDKE into one with a diminishing bias. It involves the use of an a-priori estimate of the measurement error in the samples. This is not that unreasonable since most systems of measurement have some kind of estimate to the measurement error. Since the sample covariance matrix \mathbf{C} is the only biased term in the equation for the GDKE center, this is what will be altered.

5.1.1 Derivation

The derivation stems from a simple substitution. The substitution

$$(171) \quad \mathbf{C}' = \mathbf{C} - \hat{\Sigma}$$

has the convenient property of

$$(172) \quad E(\mathbf{C}') = \mathbf{C}_0 + \Sigma - \hat{\Sigma}$$

If the true measurement covariance is the same as the estimated measurement covariance then

$$(173) \quad E(\mathbf{C}') = \mathbf{C}_0$$

The covariance of the new sample covariance matrix is the same as the old one since we are just adding a constant to the variable.

$$(174) \quad Cov(\mathbf{C}'_{ij}, \mathbf{C}'_{mn}) = Cov(\mathbf{C}_{ij}, \mathbf{C}_{mn})$$

if the error estimate is the same as the truth error covariance.

Inserting Equation (171) will produce the following equations for the solution of a hypersphere

$$(175) \quad \hat{c}' = \bar{x} + \frac{1}{2} \mathbf{C}'^{-1} \mathbf{S}$$

The radius estimator can be similarly compensated for its bias by

$$(176) \quad \hat{r}' = \sqrt{\frac{N-1}{N} Tr(\mathbf{C}') + (\bar{x} - \hat{c}')^T (\bar{x} - \hat{c}')}$$

where $Tr(*)$ means the trace of the matrix.

So where does this estimate of the measurement covariance come from? An unbiased estimator for the trace of the measurement covariance is presented below which relies on known information about the sphere being measured.

$$(177) \quad Tr(\hat{\Sigma}) = \frac{1}{N} \sum_{i=1}^N (x_i - c_0)^T (x_i - c_0) - r_0^2$$

During calibration (i.e. finding the measurement error), a known sphere with radius and center can be measured, providing the estimate of the trace of the measurement covariance.

5.1.2 Statistical Properties

Now it is desirable to find the statistical properties of the new estimators and compare them to the old GDKE. If the estimate is equal to the true sample covariance then these new equations have the following statistical properties. The altered covariance is expanded by the Leontief inverse as

$$(178) \quad \mathbf{C}'^{-1} = \mathbf{C}_0^{-1} + \sum_{k=1}^{\infty} (\mathbf{I} - \mathbf{C}_0^{-1} \mathbf{C}')^k \mathbf{C}_0^{-1}$$

Using this expansion, the altered center estimator is

$$(179) \quad \hat{c}' = \bar{x} + \frac{1}{2} \mathbf{C}_0^{-1} \mathbf{S} + \frac{1}{2} \sum_{k=1}^{\infty} (\mathbf{I} - \mathbf{C}_0^{-1} \mathbf{C}')^k \mathbf{C}_0^{-1} \mathbf{S}$$

The expectation of the altered center estimator is

$$(180) \quad E(\hat{c}') = \bar{\mu} + \frac{1}{2} \mathbf{C}_0^{-1} \mathbf{S}_0 + \frac{1}{2} \sum_{k=1}^{\infty} E\left((\mathbf{I} - \mathbf{C}_0^{-1} \mathbf{C}')^k \mathbf{C}_0^{-1} \mathbf{S}\right)$$

Using the same analysis for the GDKE in the previous section, the new estimator has an expectation of

$$(181) \quad E(\hat{c}') = c_0 - \frac{1}{2} \mathbf{C}_0^{-1} \Delta \mathbf{S} + \frac{1}{2} \sum_{k=2}^{\infty} (-\mathbf{C}_0^{-1} \Delta \mathbf{C})^k \mathbf{C}_0^{-1} (\mathbf{S}_0 + \Delta \mathbf{S})$$

Then, the bias of the new estimator is exposed as

$$(182) \quad E(\hat{c}') = c_0 + O\left(\frac{1}{\sqrt{N}} \sigma \mathbf{C}_0^{-1} \sqrt{\mathbf{F}_0}\right)$$

The covariance of the new center estimator, with similar analysis, is

$$(183) \quad \text{Cov}(\hat{c}', \hat{c}'^T) = \frac{1}{N} \sigma^2 \mathbf{C}_0^{-1} \left(8\mathbf{F}_0 + \text{Tr}(\mathbf{F}_0) - 4\text{Tr}(\mathbf{C}_0)\mathbf{C}_0 - \text{Tr}(\mathbf{C}_0)^2 \right) \mathbf{C}_0^{-1} + \mathcal{O}\left(\frac{\sigma^4}{N}\right)$$

The expectation of the square of the new radius estimator is

$$(184) \quad E(\hat{r}'^2) = r_0^2 + \mathcal{O}\left(\frac{1}{\sqrt{N}} \sigma \bar{\mu}^T \mathbf{C}_0^{-1} \sqrt{\mathbf{F}_0}\right)$$

The variance of the radius estimator comes to

$$(185) \quad \text{Var}(\hat{r}'^2) = \mathcal{O}\left(\frac{1}{N} \Sigma\right)$$

The expectation of the measurement covariance estimator is simply

$$(186) \quad E\left(\text{Tr}(\hat{\Sigma})\right) = \text{Tr}(\Sigma)$$

The variance of the measurement covariance estimator is found from the expectation of the square. Starting from the square

$$(187) \quad \begin{aligned} \text{Tr}(\hat{\Sigma})^2 &= (r_0^2 - c_0^T c_0)^2 + 4(r_0^2 - c_0^T c_0) c_0^T \bar{x} + 4c_0^T \bar{x} \bar{x}^T c_0 - 4c_0^T \frac{1}{N^2} \sum_{i=1}^N \sum_{j=1}^N x_j x_i^T x_i \\ &+ 2(c_0^T c_0 - r_0^2) \frac{1}{N} \sum_{i=1}^N x_i^T x_i + \frac{1}{N^2} \sum_{i=1}^N \sum_{j=1}^N x_i^T x_i x_j^T x_j \end{aligned}$$

The expectation of this square is

$$(188) \quad \begin{aligned} E\left(\text{Tr}(\hat{\Sigma})^2\right) &= \left(r_0^2 - c_0^T c_0 - \text{Tr}(\Sigma) + 4c_0^T \bar{\mu} - 2 \frac{1}{N} \sum_{i=1}^N \mu_i^T \mu_i \right) \left(r_0^2 - c_0^T c_0 - \text{Tr}(\Sigma) \right) \\ &+ 4c_0^T \bar{\mu} \left(\bar{\mu}^T c_0 - \frac{1}{N} \sum_{i=1}^N \mu_i^T \mu_i \right) + 4 \frac{1}{N} c_0^T \Sigma c_0 - 8 \frac{1}{N} c_0^T \Sigma \bar{\mu} \\ &+ \left(\frac{1}{N} \sum_{i=1}^N \mu_i^T \mu_i \right)^2 \\ &+ 2 \frac{1}{N} \text{Tr}(\Sigma^2) + 4 \frac{1}{N^2} \sum_{i=1}^N \mu_i^T \Sigma \mu_i \end{aligned}$$

This expectation turns the variance into

$$(189) \quad \text{Var}\left(\text{Tr}(\hat{\Sigma})\right) = 2\frac{1}{N}\left(\text{Tr}(\Sigma^2) + 2\frac{1}{N}\sum_{i=1}^N(\mu_i - c_0)^T \Sigma(\mu_i - c_0)\right)$$

If the measurement covariance is expected to be diagonal ($\Sigma = \sigma^2 \mathbf{I}$) then the variance of the variance estimator is

$$(190) \quad \text{Var}(\hat{\sigma}^2) = 2\frac{1}{ND^2}\sigma^2(D\sigma^2 + 2r_0^2)$$

where D is the dimension of the measurement. A typical use of these new estimators can be displayed using Mathematica, with exactly the same data as was displayed for the GDKE in Figure 17.

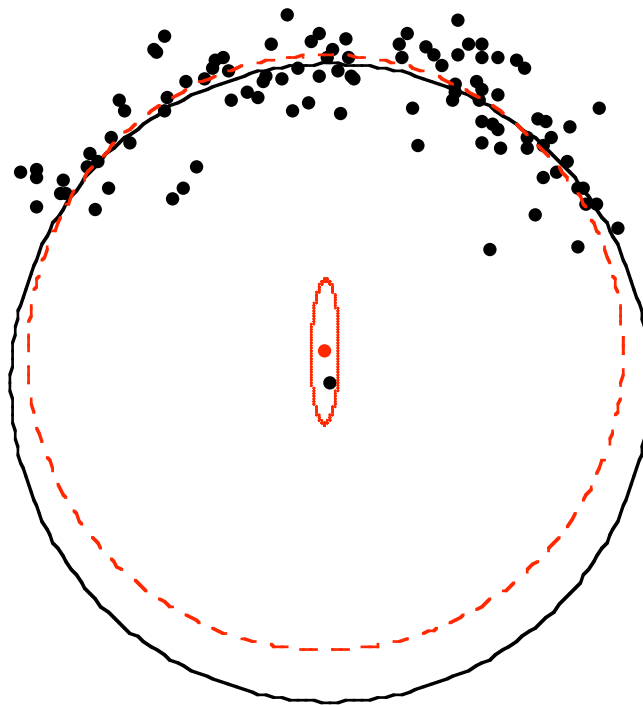


Figure 18 UGDK Error Ellipse

As can be seen in Figure 18, the true center is within the error ellipsoid. This data contains 100 points generated with a diagonal measurement covariance with all diagonals

equal to 0.05^2 . The Leontief condition ($\rho < 1$) is satisfied with the spectral radius in question equal to 0.557238.

These equations show that there still is a bias, but it is asymptotically unbiased. Figure 19 shows a Monte-Carlo run that explicitly shows the $1/\sqrt{N}$ dependency. The error in the estimate is compared with how many points were analyzed for a particular joint in some motion capture data.

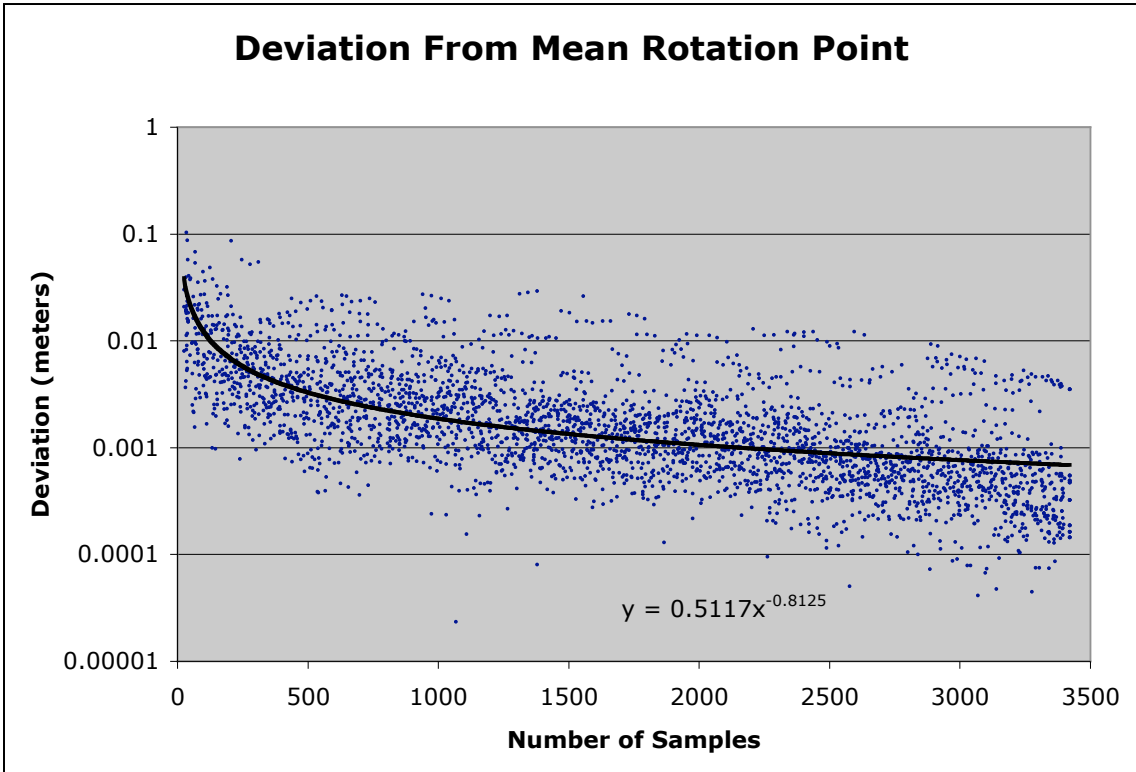


Figure 19 Sample Size Dependency of Deviation

An example analysis using MLE, UGDK and GDKE is presented in Figure 20. The figure clearly shows the improvement over the GDKE. The figure shows the bias is removed using the UGDK.

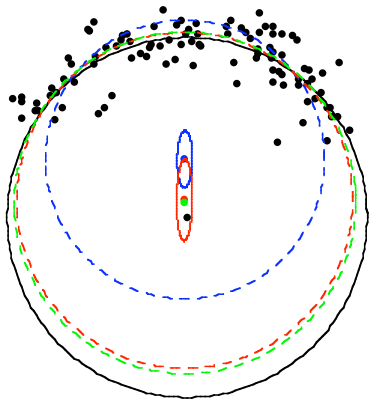


Figure 20 One hundred samples comparison of MLE (green), UGDK (red), GDKE (blue)

There is a case where this new method fails to bring an improvement. The case is not very common and should not be of concern. The following graph shows the problem.

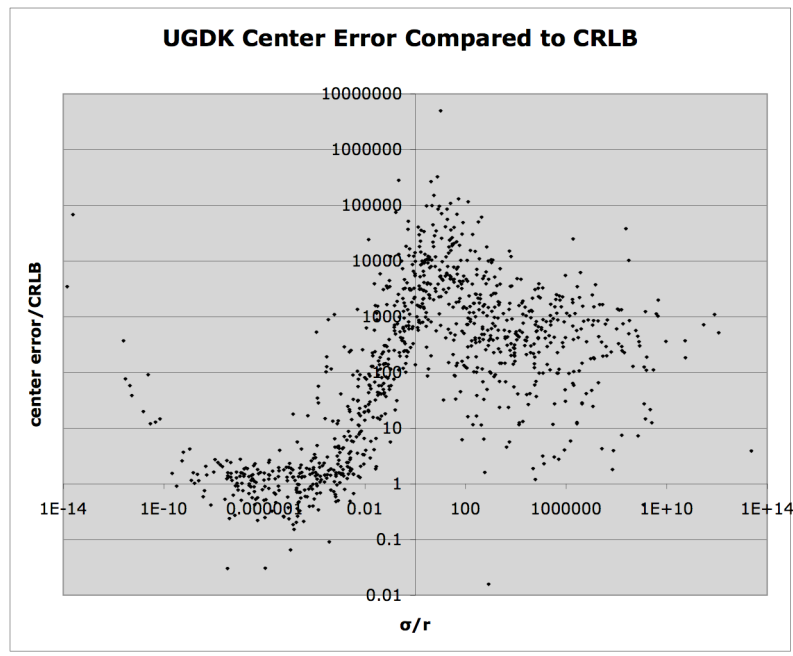


Figure 21 UGDK Compared to CRLB

There is no concern here since all of the methods have troubles in this area. This situation is a bit impractical, as no one wants a system whose measurement error is actually bigger than the item being measured?

That brings up the point - when should a measurement system be trusted? A cursory glance would say

$$(191) \quad \sigma < r_0$$

is when the system should be accepted. Upon further analysis, the answer comes from the world of economics [101] - the Leontief inverse.

$$(192) \quad (\mathbf{I} - \mathbf{A})^{-1} = \mathbf{I} + \mathbf{A} + \mathbf{A}^2 + \mathbf{A}^3 + \dots$$

This series expansion is convergent when the spectral radius (i.e. largest absolute eigenvalue) is

$$(193) \quad \rho(\mathbf{A}) < 1$$

The matrix of interest in our application is the sample covariance matrix \mathbf{C} . The matrix can be expanded two ways. The first way is of practical importance and that is when

$$(194) \quad \rho(\mathbf{C}_0^{-1}\Sigma) < 1$$

which allows us to expand the inverse of the expectation of the covariance matrix into

$$(195) \quad (\mathbf{C}_0 + \Sigma)^{-1} = \mathbf{C}_0^{-1} - \mathbf{C}_0^{-1}\Sigma\mathbf{C}_0^{-1} + (\mathbf{C}_0^{-1}\Sigma)^2\mathbf{C}_0^{-1} - \dots$$

If the spectral radius is greater than one, then the expansion turns into

$$(196) \quad (\mathbf{C}_0 + \Sigma)^{-1} = \Sigma^{-1} - \Sigma^{-1}\mathbf{C}_0\Sigma^{-1} + (\Sigma^{-1}\mathbf{C}_0)^2\Sigma^{-1} - \dots$$

So what is this magical turning point? If the measurement covariance Σ is diagonal with equal variances in all directions (i.e. $\Sigma = \sigma^2\mathbf{I}$) then the spectral radius can be evaluated as

$$(197) \quad \rho(\mathbf{C}_0^{-1}\Sigma) = \frac{\sigma^2}{\lambda_{\min}}$$

The where λ_{\min} is the smallest eigenvalue of the sample covariance matrix \mathbf{C}_0 . This is still not very useful because eigenvalues are mathematically intensive to solve. Let us set up a scenario to produce an answer for the limiting case of too many data points. We want to develop an equation for the eigenvalues when the hypersphere is partially covered by sample points.

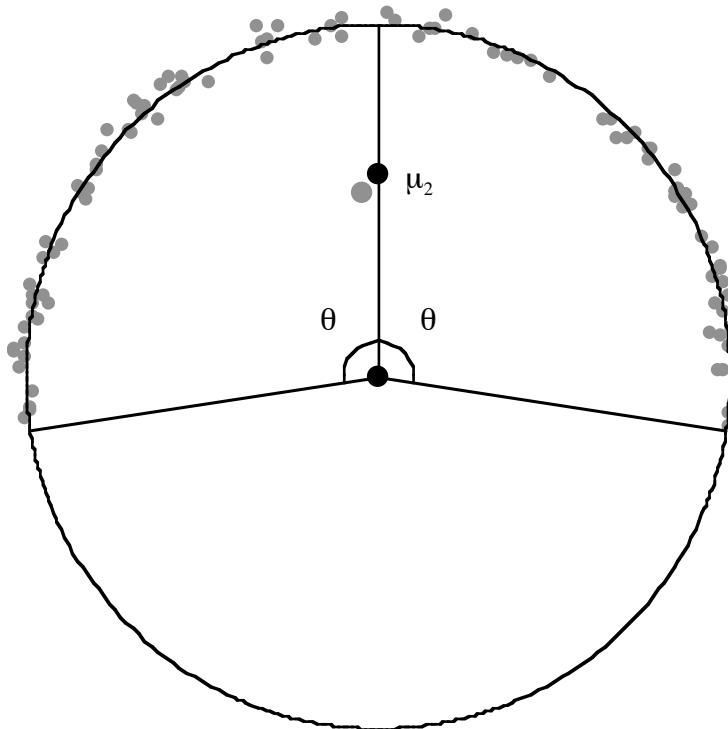


Figure 22 Circle with Constrained Data

First is the case for a two-dimensional hypersphere (i.e. circle). The points are confined to an angular distance θ from the y-axis. Each point on the circle can be expressed as

$$(198) \quad v_2 = \begin{pmatrix} r_0 \sin a \\ r_0 \cos a \end{pmatrix}$$

where a is the angle from the y-axis. The mean has an asymptote as the number of samples increase.

$$(199) \quad \mu_2 = \lim_{N \rightarrow \infty} \frac{1}{N} \sum_{i=1}^N v_2 = \frac{1}{\phi_2} \int_{-\theta}^{\theta} v_2 da$$

where

$$(200) \quad \phi_2 = \int_{-\theta}^{\theta} da = 2\theta$$

This gives us the answer of the asymptotic average being on the y-axis at

$$(201) \quad \mu_2 = r_0 \frac{\sin \theta}{\theta} \begin{pmatrix} 0 \\ 1 \end{pmatrix}$$

Similarly, the asymptotic covariance can be found as the integral

$$(202) \quad \mathbf{C}_2 = \frac{1}{\phi_2} \int_{-\theta}^{\theta} (v_2 - \mu_2)(v_2 - \mu_2)^T da = \begin{pmatrix} \lambda_{\max 2} & 0 \\ 0 & \lambda_{\min 2} \end{pmatrix}$$

This matrix happens to be diagonal containing all of the eigenvalues which turn out to be

$$(203) \quad \lambda_{\min 2} = r_0^2 \frac{\theta(2\theta + \sin(2\theta)) - 4 \sin^2 \theta}{4\theta^2} \text{ and}$$

$$(204) \quad \lambda_{\max 2} = r_0^2 \frac{\theta - \cos \theta \sin \theta}{2\theta}$$

The three-dimensional hypersphere (i.e. sphere) is similarly evaluated only this time, the solid angle must be integrated. The points are confined to an angular distance θ from the z-axis. The point on the sphere is

$$(205) \quad v_3 = \begin{pmatrix} r_0 \sin a \cos b \\ r_0 \sin a \sin b \\ r_0 \cos a \end{pmatrix}$$

The asymptotic limit of the average point is then

$$(206) \quad \mu_3 = \frac{1}{\phi_3} \int_0^\theta \int_0^{2\pi} v_3 \sin a \, db \, da$$

where

$$(207) \quad \phi_3 = \int_0^\theta \int_0^{2\pi} \sin a \, db \, da = 2\pi(1 - \cos\theta)$$

The asymptotic limit of the average lies on the z-axis at

$$(208) \quad \mu_3 = r_0 \cos^2\left(\frac{\theta}{2}\right) \begin{pmatrix} 0 \\ 0 \\ 1 \end{pmatrix}$$

Similarly, the asymptotic covariance is evaluated as

$$(209) \quad \mathbf{C}_3 = \frac{1}{\phi_3} \int_0^\theta \int_0^{2\pi} (v_3 - \mu_3)(v_3 - \mu_3)^T \sin a \, db \, da = \begin{pmatrix} \lambda_{\max 3} & 0 & 0 \\ 0 & \lambda_{\max 3} & 0 \\ 0 & 0 & \lambda_{\min 3} \end{pmatrix}$$

The diagonals of this matrix have two equal eigenvalues (the largest) and one smallest value.

$$(210) \quad \lambda_{\min 3} = r_0^2 \frac{1}{3} \sin^4\left(\frac{\theta}{2}\right) \text{ and}$$

$$(211) \quad \lambda_{\max 3} = r_0^2 \frac{1}{3} (2 + \cos\theta) \sin^2\left(\frac{\theta}{2}\right)$$

Following this answer, a good measurement condition for the sphere is when

$$(212) \quad \sigma < r_0 \frac{1}{\sqrt{3}} \sin^2\left(\frac{\theta}{2}\right)$$

whereas the best condition to get a good answer for a circle is when

$$(213) \quad \sigma < r_0 \frac{\sqrt{\theta(2\theta + \sin(2\theta)) - 4 \sin^2 \theta}}{2\theta}$$

5.2 Cylindrical Joint Solution

Special considerations are needed when a cylindrical joint is suspected. In this case, a point on the upper segment will always draw a circular arc thereby remaining planar. Any method for finding a sphere where only a circle exists will fail. The planar condition can be discovered when the sample covariance matrix \mathbf{C} becomes near singular:

$$(214) \quad |\mathbf{C}| \approx 0$$

This occurs when the rank of \mathbf{C} is less than the number of dimensions. In essence, one dimension must be removed from the sphere equation to get the circle estimation. The sample covariance matrix can be rewritten using its eigensystem values.

$$(215) \quad \mathbf{C} = \sum_{i=1}^D \lambda_i \mathbf{v}_i \mathbf{v}_i^T$$

where λ_i are the eigenvalues and \mathbf{v}_i are the corresponding unit eigenvectors. The inverse of the matrix can be similarly expanded with the same eigensystem as

$$(216) \quad \mathbf{C}^{-1} = \sum_{i=1}^D \frac{1}{\lambda_i} \mathbf{v}_i \mathbf{v}_i^T$$

The GDKE solution to the circle in 3D space can be calculated two ways. The first way does not involve inverting small values. This is achieved by removing the eigenvalues that are below a certain limit. This reduced matrix can then be used in the GDKE formula producing

$$(217) \quad \hat{\mathbf{c}} = \bar{\mathbf{x}} + \frac{1}{2} \sum_{\lambda_i > \varepsilon} \frac{1}{\lambda_i} \mathbf{v}_i \mathbf{v}_i^T \mathbf{S}$$

$$(218) \quad \hat{r} = \sqrt{\sum_{\lambda_i > \varepsilon} \frac{1}{4\lambda_i^2} (\mathbf{v}_i^T \mathbf{S})^2 + \frac{N-1}{N} \lambda_i}$$

This new center is the best-fit estimate of a circle for the data. This equation is successful even if the sample covariance is exactly singular. This formula can be used to calculate the center and radius of curvature for curvilinear paths in any dimensional space. For the rotation point of a joint, it has a flaw. A cylindrical joint rotates about an axis. The center that is calculated lies on this axis but might not be the volumetric center of the cylinder. To overcome this, two markers on either side of the center can be averaged.

5.3 Multiple Marker Solution

For multiple markers going around the same center of rotation, another formula can be achieved by the same analysis of least squares. This technique is good to use when more than one marker is available. It has the ability to average out errors when one marker is too close to the rotation point or has other systematic problems. The gradient of the sum of variances (cf. Equation (85)) is

$$(219) \quad \nabla S_m^2 = \sum_{p=1}^M 4 \left(2\mathbf{C}_p (\hat{\mathbf{c}}_m - \bar{\mathbf{x}}_p) - \mathbf{S}_p \right)$$

where M is the number of markers. Setting this to zero will provide a solution for multiple markers:

$$(220) \quad \hat{\mathbf{c}}_m = \left(\sum_{p=1}^M \mathbf{C}_p \right)^{-1} \sum_{p=1}^M \mathbf{C}_p \bar{\mathbf{x}}_p + \frac{1}{2} \mathbf{S}_p$$

and the individual radius becomes

$$(221) \quad \hat{r}_p = \sqrt{\frac{N-1}{N} \text{Tr}(\mathbf{C}_p) + (\bar{x}_p - \hat{c}_m)^T (\bar{x}_p - \hat{c}_m)}$$

where M is the number of markers and the subscript p indicates values that utilize the single marker's positions.

The same unbiased analysis applies to this multiple marker version and results in

$$(222) \quad \hat{c}'_m = \left(\sum_{p=1}^M \mathbf{C}'_p \right)^{-1} \sum_{p=1}^M \mathbf{C}'_p \bar{x}_p + \frac{1}{2} \mathbf{S}_p \text{ and}$$

$$(223) \quad \hat{r}'_p = \sqrt{\frac{N-1}{N} \text{Tr}(\mathbf{C}'_p) + (\bar{x}_p - \hat{c}'_m)^T (\bar{x}_p - \hat{c}'_m)}.$$

The matrix that is to be inverted here is still a positive-definite matrix since positive-definite matrices added together still produce a positive-definite matrix. This allows for the speedier Cholesky decomposition just like before. The singular values can be excluded just like in Chapter 5.2. An example of the MGDK method is presented in Figure 23.

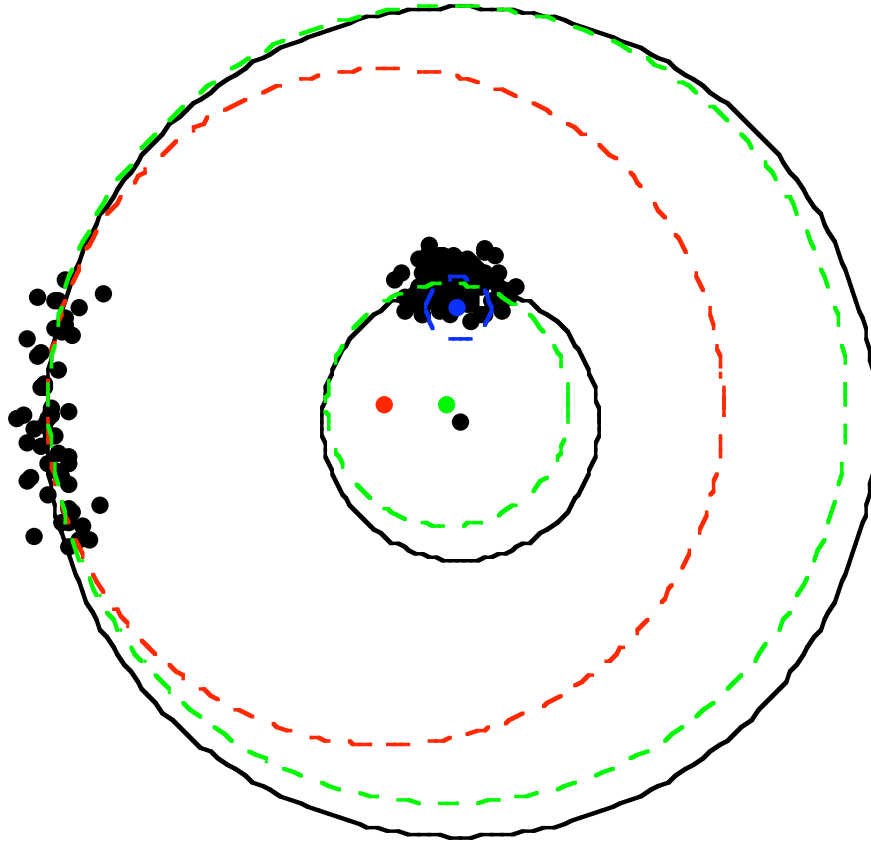


Figure 23 MGDK example

This example shows what happens when the individual circles are compared to that when combined in the MGDK. The outer circle solution is drawn in red; the inner circle solution is drawn in blue, and the MGDK solution is drawn in green. The example shows a dramatic improvement over both of the individual circle calculations.

5.4 Incrementally Improved Solution

A more refined answer can be achieved when using an incremental improvement formula. The idea here is a group of samples are collected and an answer is retrieved

from the GDKE or UGDK formulae. Then a new sample is added, refining the previous answer for the center. Starting off simple, the mean has a recursion of

$$(224) \quad \bar{x}_{n+1} = \bar{x}_n + \frac{x_{n+1} - \bar{x}_n}{n+1}, \quad \bar{x}_1 = x_1$$

One definition will make the following equations smaller:

$$(225) \quad \delta_n \equiv x_n - \bar{x}_n$$

$$(226) \quad \delta_{n+1} = n(\bar{x}_{n+1} - \bar{x}_n)$$

The sample covariance matrix has a recurrence relationship of

$$(227) \quad \mathbf{C}_{n+1} = \frac{n-1}{n} \mathbf{C}_n + \frac{n+1}{n^2} \delta_{n+1} \delta_{n+1}^T, \quad \mathbf{C}_1 = \mathbf{0}$$

The unbiased improvement of the sample covariance matrix is

$$(228) \quad \mathbf{C}'_{n+1} = \frac{n-1}{n} \mathbf{C}'_n - \frac{1}{n} \hat{\Sigma} + \frac{n+1}{n^2} \delta_{n+1} \delta_{n+1}^T, \quad \mathbf{C}'_1 = \mathbf{0}$$

The inverse of the covariance matrix also has a recurrence - without doing an additional matrix inverse

$$(229) \quad \mathbf{C}_{n+1}^{-1} = \frac{n}{n-1} \mathbf{C}_n^{-1} \left(\mathbf{I} + \frac{\delta_{n+1} \delta_{n+1}^T \mathbf{C}_n^{-1}}{\frac{n(n-1)}{n+1} + \text{Tr}(\delta_{n+1} \delta_{n+1}^T \mathbf{C}_n^{-1})} \right)$$

Putting these together produces a recurrence relationship for the center of the hypersphere

$$(230) \quad \mathbf{S}_{n+1} = \frac{n-1}{n} \mathbf{S}_n + \frac{1}{n} \left(-2\mathbf{C}_{n+1} - \text{Tr}(\mathbf{C}_{n+1}) + \frac{(n+1)(n+2)}{n^2} \delta_{n+1} \delta_{n+1}^T \right) \delta_{n+1}$$

$$(231) \quad \hat{c}_{n+1} = \bar{x}_{n+1} + \frac{1}{2} \mathbf{C}_{n+1}^{-1} \mathbf{S}_{n+1}$$

$$(232) \quad \hat{r}_{n+1}^2 = \frac{n}{n+1} \text{Tr}(\mathbf{C}_{n+1}) + (\bar{x}_{n+1} - \hat{c}_{n+1})^T (\bar{x}_{n+1} - \hat{c}_{n+1})$$

The cost of the incremental improvement to produce the new center and radius is measured in the FLOP count:

$$(233) \quad FLOPs = 17\frac{1}{2}D^2 + 23\frac{1}{2}D + 12$$

For a sphere, the FLOPs are 123 for every new point. When compared to the FLOPs for the GDKE method, this incremental approach is about four times slower. This makes the incremental approach a last resort when a few extra points need to be added to a previously calculated center and radius. This new estimator has the distinct advantage of constant memory requirements no matter how many points are analyzed.